Supplementary Information

Gut stem cell aging is driven by mTORC1 via a p38 MAPK-p53 pathway
Dan He et al.

Supplementary Figure 1

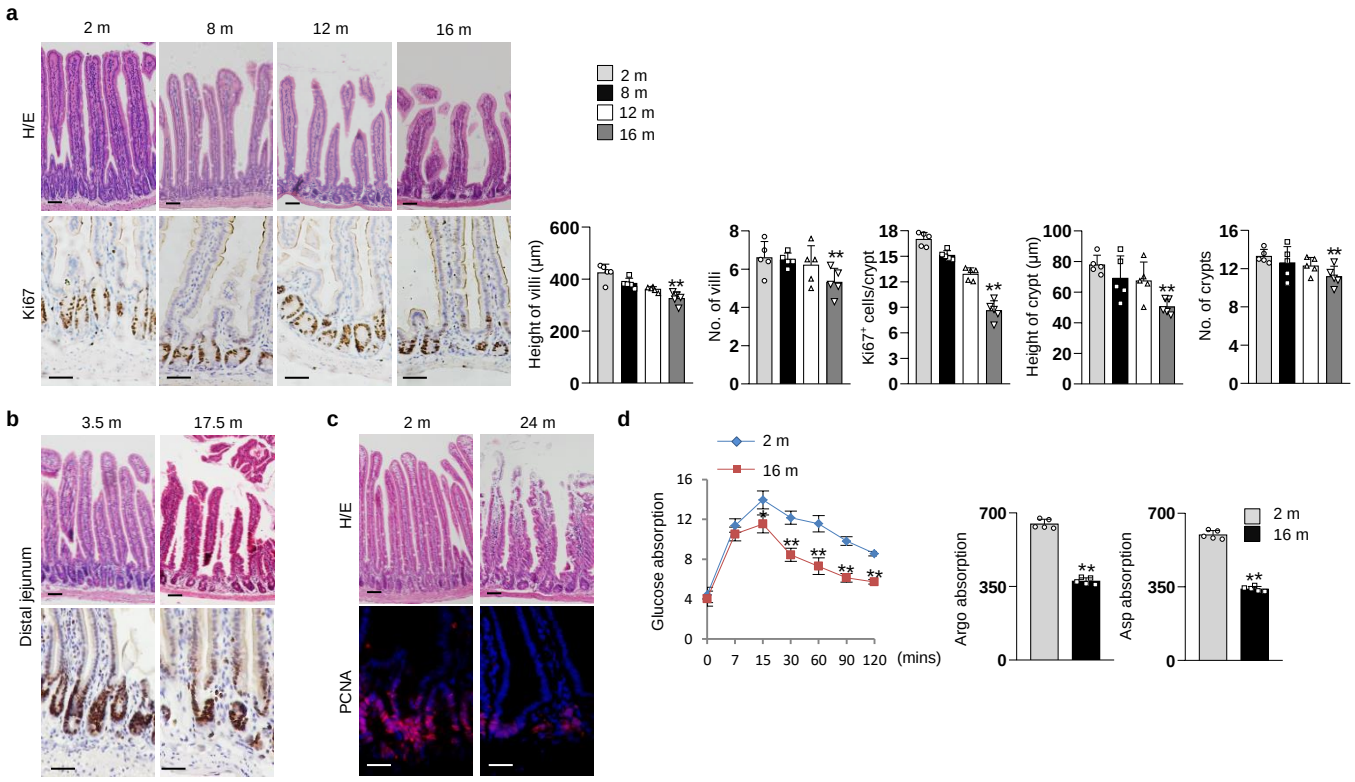


**Supplementary Figure 1. Old mice showed defects in villus/crypt structure and nutrient absorbing activities.**
(a). Comparison of villus structure and TA cell proliferation of 2-, 8-, 12-, and 16-month old mice. The proximal jejunum samples were sectioned and stained with H/E or Ki67 antibodies. Right panels: quantitation data (mean ± SEM). N=5 mice per group. **p<0.01 (determined using Student's *t*-test). (b). Comparison of the distal jejunum of 3.5 and 17.5-month old mice. (c). Comparison of the proximal jejunum of 3.5 and 24-month old mice. (d). Sixteen-month-old mice showed a decrease in nutrient absorbing activities for glucose and amino acids (arginine and aspartic acid). Data are expressed as mean ± SEM. N=5 mice per group. *p<0.05, **p<0.01 (determined using Student's *t*-test).

# Supplementary Figure 2

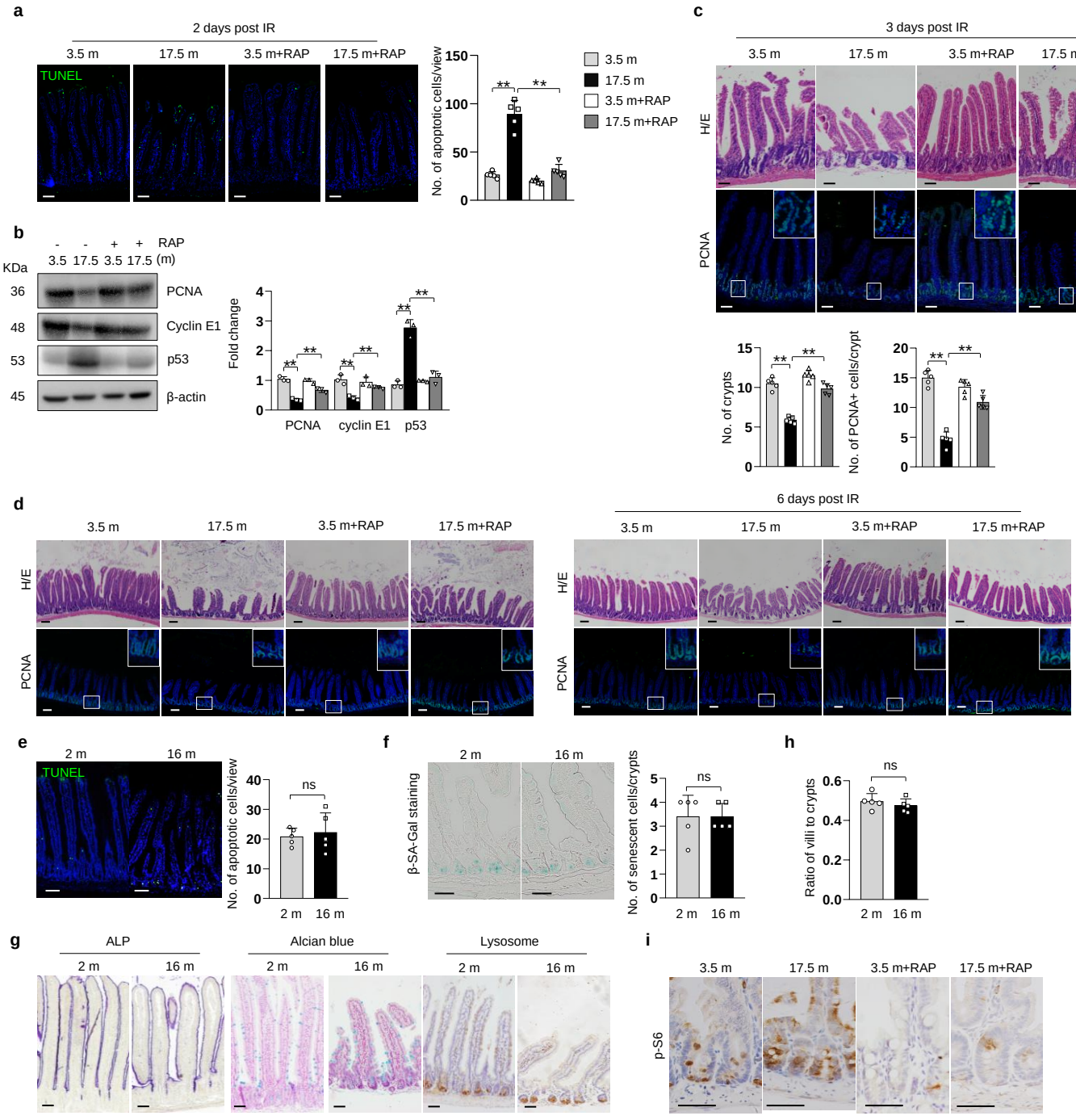


**Supplementary Figure 2. mTOR activation increases sensitivity to IR in villi/crypts of geriatric mice.**
(a). Seventeen and half-month-old mice showed an increase in apoptotic cells 2 days after IR, which was rescued by RAP. Right panels: quantification data (mean ± SEM). N=5 mice per group. **p<0.01 (determined using Student's *t*-test). (b). The intestine samples of 17.5-month-old mice showed decreases in PCNA and cyclin E and an increase in p53 in crypt samples at day 2 after IR, which was rescued by RAP. Right panel: quantitation data (mean ± SEM). N=5 mice per group. ** p<0.01 (determined using Student's *t*-test). (c). Seventeen and half-month-old mice showed increased sensitivity to IR-induced decreases in the numbers of crypts and proliferating cells compared to young mice at day 3 post IR, which were partially rescued by 1.5 months of RAP treatment (3 mg/kg body weight) starting at 16 months of age. Bottom panels: quantitation data (mean ± SEM). N=5 mice per group. **p<0.01 (determined using Student's *t*-test). (d). Lower magnification images of intestinal sections of 3.5 and 17.5-month-old mice (left panel) and villus regeneration in these mice at day 6 post IR (right panel). (e-h). No difference was observed between 2- and 16-month-old mice in the percentage of apoptotic cells (e) or SA-β-Gal senescent cells (f) in the villi, differentiation of villus cells (g), or the villus-to-crypt ratios (h). N=5. ns, not significant. (i). mTORC1 activation was inhibited by RAP treatment. The 16-month-old mice were sacrificed after 1.5 months of RAP treatment and the proximal jejunum sections were stained for p-S6.

# Supplementary Figure 3

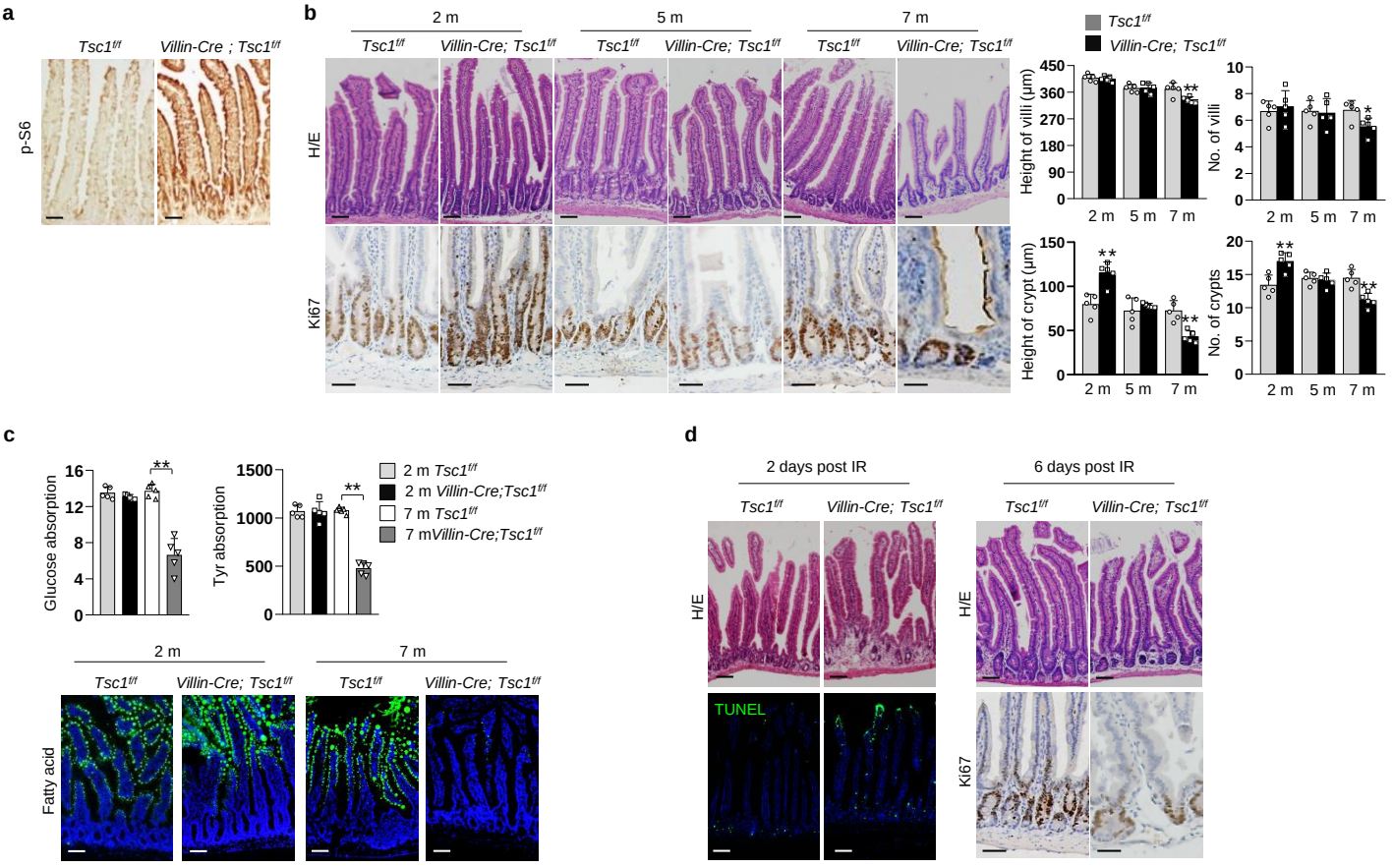


**Supplementary Figure 3. Ablation of *Tsc1* in enterocytes induces villus premature aging.**
(a). Immunostaining of p-S6 showed that *Villin-Cre; Tsc1$^{f/f}$* mouse intestine sections displayed enhanced mTORC1 activation. (b). Two-month-old *Villin-Cre; Tsc1$^{f/f}$* mice showed a villus/crypt overgrowth phenotype, 5-month-old mutant mice showed villi similar to age-matched wild type mice, and 7-month-old mutant mice showed aging-like change in villus structure. Right panels: quantitation data (mean ± SEM). N=5 mice per group. *p<0.05, **p<0.01 (determined using Student's *t*-test). (c). *Villin-Cre; Tsc1$^{f/f}$* mice showed defects in nutrient absorption activities at 7 months of age. Data are expressed as mean ± SEM. N=5 mice per group. **p<0.01 (determined using Student's *t*-test). (d). *Villin-Cre; Tsc1$^{f/f}$* mice showed increased sensitivity to IR and villus regeneration defects. The 2-month-old mice were radiated at 5.0 Gy and were sacrificed 2 or 6 days later. Intestinal sections were stained with H/E, TUNEL, or anti-Ki67 antibodies.

Supplementary Figure 4

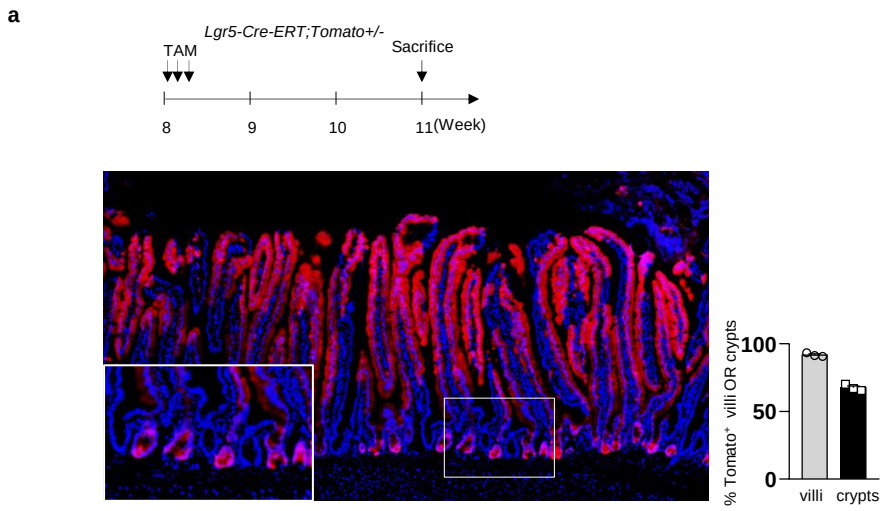


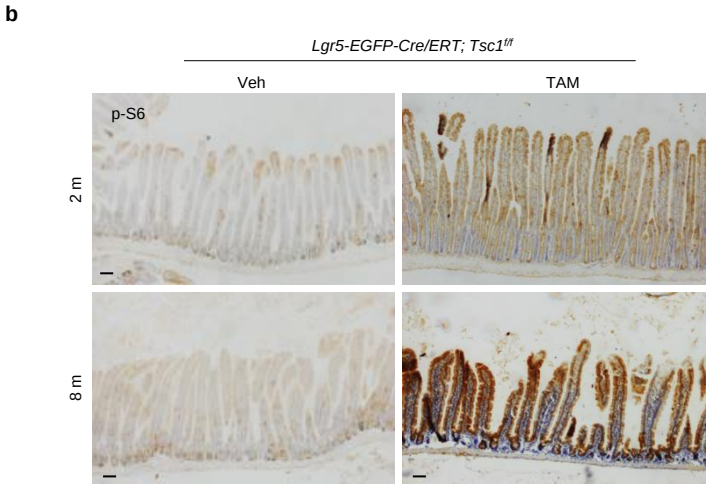


**Supplementary Figure 4. Labelling of villi in *Lgr5-CreERT; tdTomato* mice and mTORC1 activation in *Lgr5-CreERT; Tsc1$^{f/f}$* mice.**

(a). Tracing with *Lgr5-CreERT; tdTomato* mice revealed that almost all villi are labeled. One-month-old mice were administrated 3 daily doses of TAM and the mice were euthanized at 2 months of age. Right panel: quantitation data. N=3. (b). Immunostaining of p-S6 revealed that *Lgr5-Cre/ERT; Tsc1$^{f/f}$* mouse intestine sections showed enhanced mTORC1 activation 1 or 7 months after TAM treatment in almost all villi.

# Supplementary Figure 5

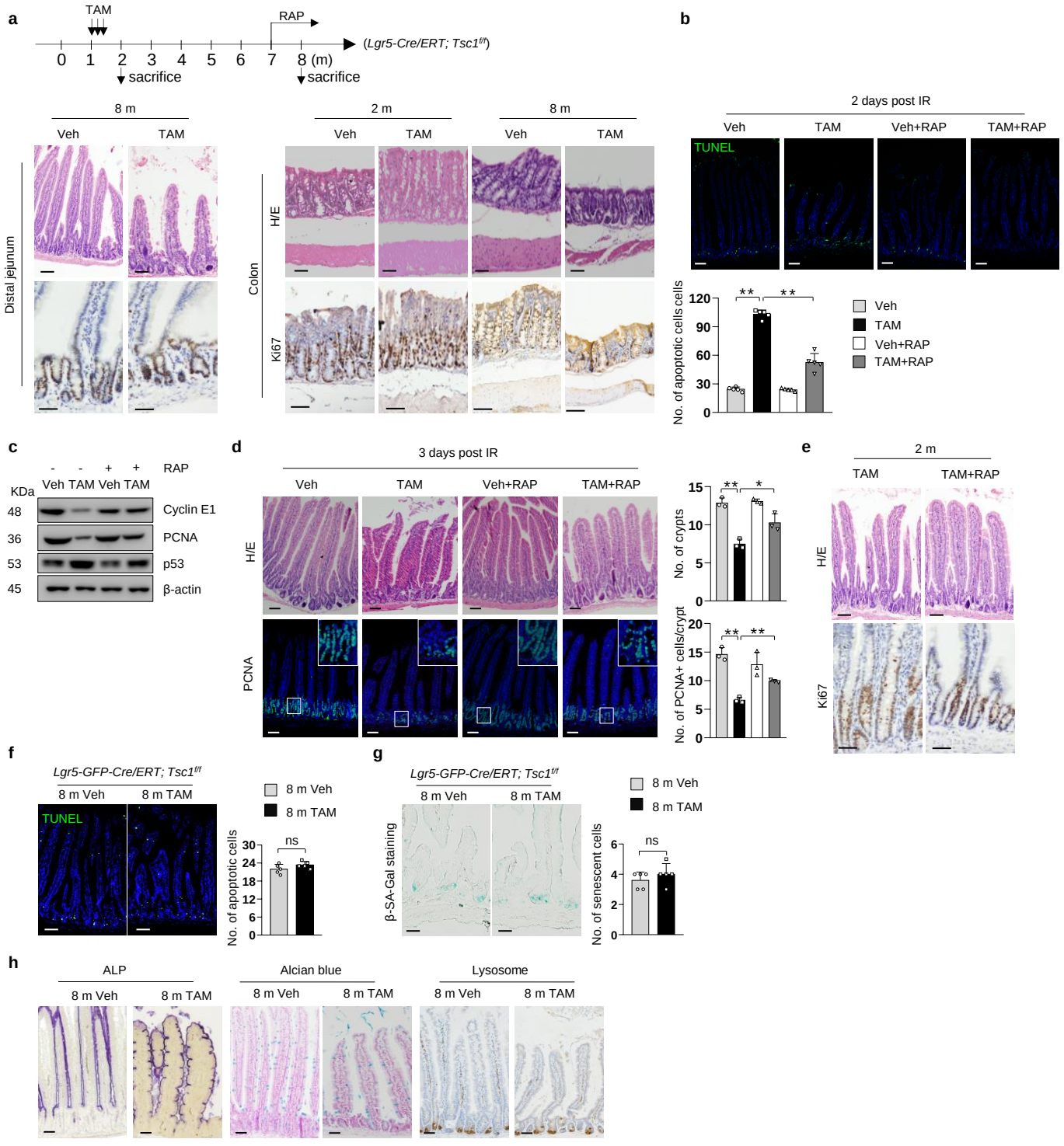


**Supplementary Figure 5. Ablation of *Tsc1* in ISCs induces villus premature aging.**
(a). H/E staining revealed that *Lgr5-Cre/ERT; Tsc1$^{f/f}$* mice showed aging of distal jejunum at 8 months of age and overgrowth of colon crypts at 2 months of age and atrophy at 8 months of age. (b). *Lgr5-Cre/ERT; Tsc1$^{f/f}$* mice showed an increase in apoptotic cells on intestinal sections 2 days after IR, which was rescued by RAP. Bottom panels: quantification data (mean ± SEM). N=5 mice per group. **p<0.01 (determined using Student's *t*-test). (c). The intestine samples of *Lgr5-Cre/ERT; Tsc1$^{f/f}$* mice showed decreases in PCNA and cyclin E and an increase in p53 in crypt samples at day 2 after IR, which was rescued by RAP. (d). *Lgr5-Cre/ERT; Tsc1$^{f/f}$* mice showed increased sensitivity to IR-induced decreases in the numbers of crypts and proliferating cells at day 3 post IR. Right panels: quantification data (mean ± SEM). N=3 mice per group. *p<0.05, **p<0.01 (determined using Student's *t*-test). (e). RAP treatment for 1 month recued the overgrowth of crypts in young *Lgr5-CreERT; Tsc1$^{f/f}$* mice. (f-h). The villi of 8-month-old *Lgr5-Cre/ERT; Tsc1$^{f/f}$* mice (TAM injected) showed no change in the number of apoptotic cells (f), β-SA-Gal positive senescent cells (g), or differentiation of villus cells (h). N=5. ns, not significant.

Supplementary Figure 6

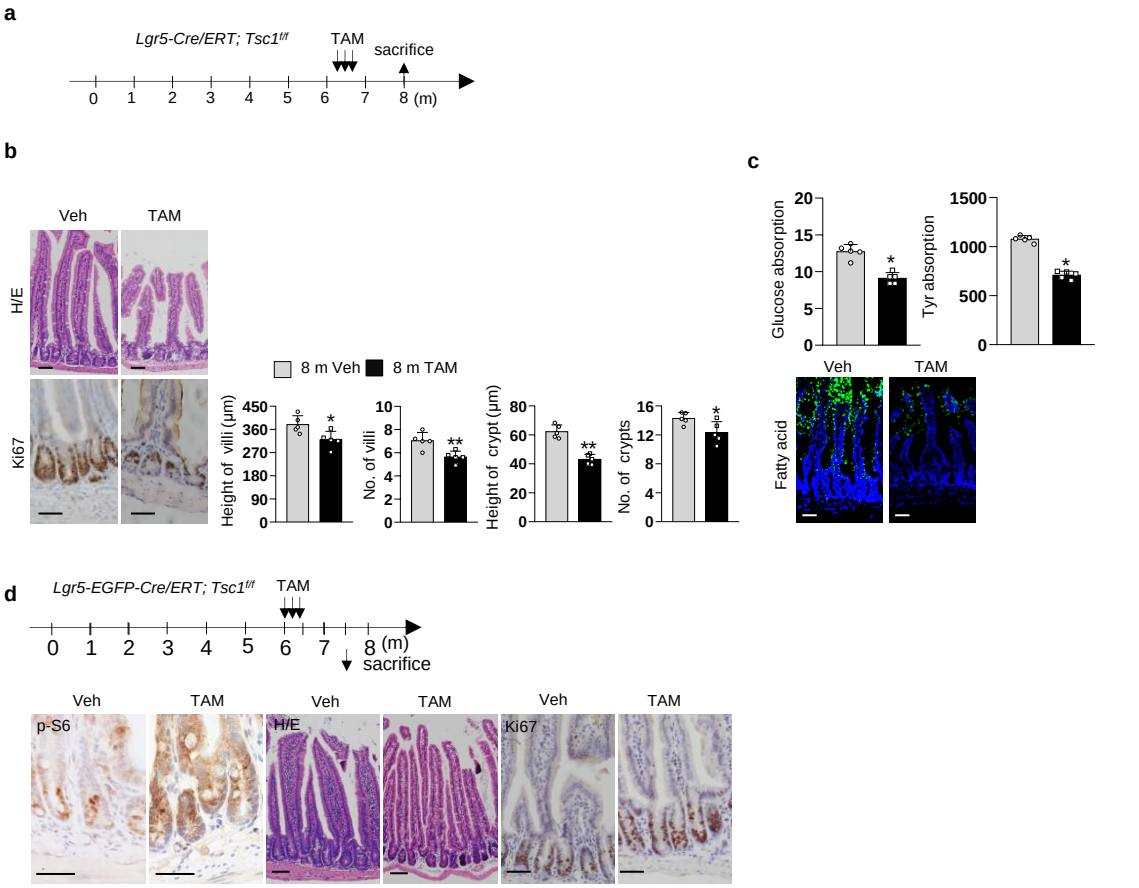


**Supplementary Figure 6. Ablation of *Tsc1* in 6.5-month-old mice induces villus premature aging.**
(a). Diagram showing the time for TAM administration (for b and c). (b,c). Ablation of *Tsc1* in 6.5-month-old mice induced defects in villus and crypt structure (b) and decreased nutrient absorption activities at 8 months of age (c). Right panels for (b): quantification data (mean ± SEM). N=5 mice per group. *p<0.05, **p<0.01 (determined using Student's *t*-test). (d). H/E staining revealed that administration of TAM to 6.5-month-old *Lgr5-Cre/ERT; Tsc1$^{f/f}$* mice did not result in overgrowth of the crypt at 7.5 months of age.

# Supplementary Figure 7

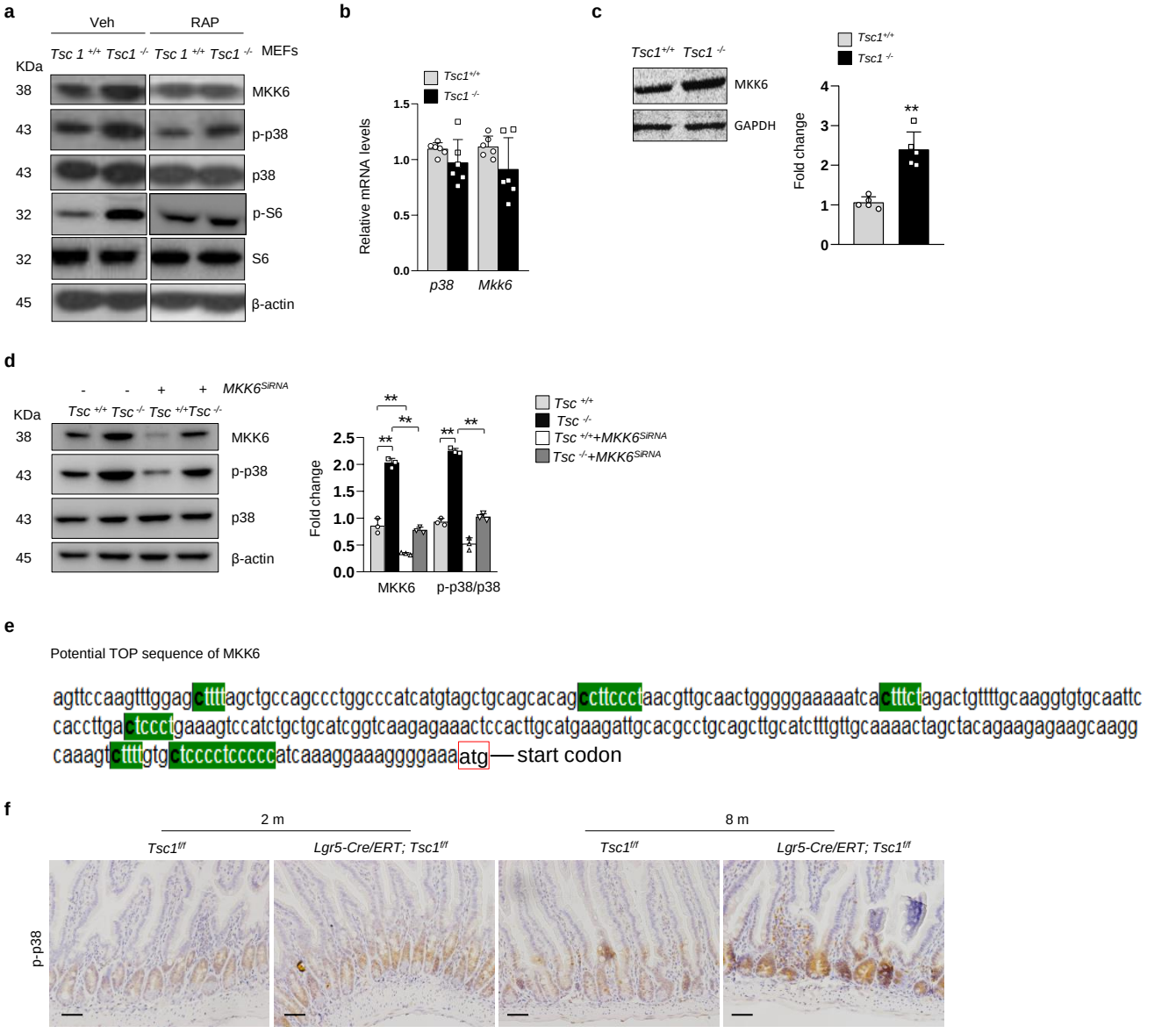


**Supplementary Figure 7. *Tsc1* deficiency leads to increased expression of MKK6 and activation of p38 MAPKs.**
(a). Western blot results revealed that *Tsc1*$^{-/-}$ MEFs showed an increase in expression of MKK6 and activation of p38 MAPKs, which were suppressed by RAP. Primary MEFs were derived from *Tsc1*$^{f/f}$ mice, infected with Cre-expressing retroviruses, selected for 3 days with puromycin, and then used for western blot analysis. (b). Quantitative PCR results showed that *Tsc1* deficiency did not significantly alter the mRNA levels of *Mkk6* in MEFs. The mRNA level of *Mkk6* of wild type cells was set at 1.0. N=6. (c). *Tsc1* deficiency increased the levels of radio-labelled MKK6 protein in MEFs. Right panel: quantitation data (mean ± SD). N=5 repetitive experiments. **p<0.01 (determined using Student's *t*-test). (d). Western blot results showed that knockdown of MKK6 led to a decrease in p38MAPK activation in *Tsc1* deficient MEFs. Right panel: quantitation data (mean ± SD). N=3 repetitive experiments. ** p<0.01, determined using Student's *t*-test. (e). Sequences of the mouse *Mkk6* 5' untranslated region. The putative TOP sequences were highlighted. (f). Immunostaining revealed that activation of p38 MAPKs was further enhanced in crypt cells of 8-month-old *Lgr5-Cre/ERT; Tsc1*$^{f/f}$ mice (TAM injected). The proximal jejunum sections were stained for p-p38 MAPKs.

# Supplementary Figure 8

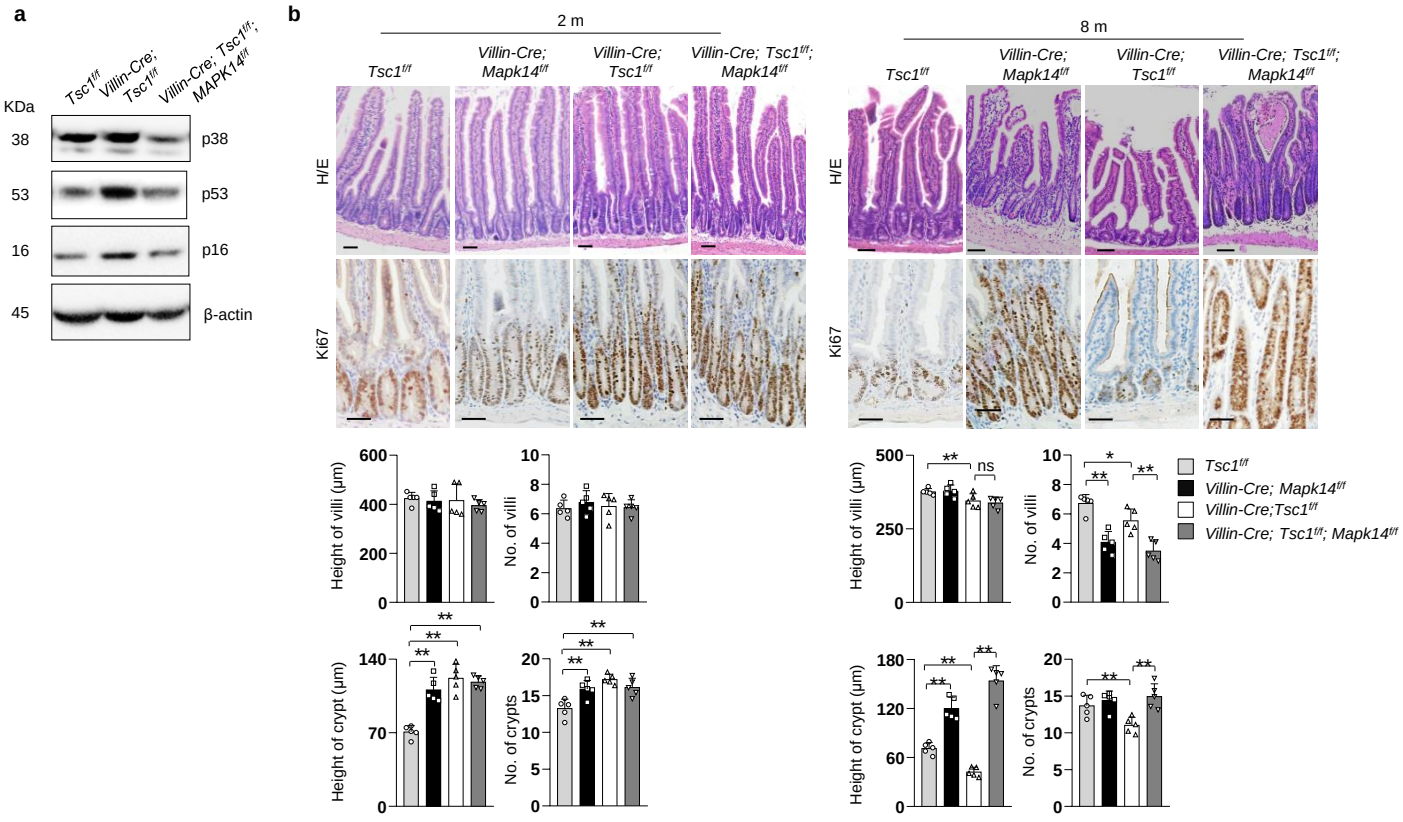


**Supplementary Figure 8. p38 MAPKs mediate the pro-aging effects of mTORC1 in *Villin-Cre; Tsc1$^{f/f}$* mice.**
(a). Western blot analysis revealed that p38α was largely deleted in small intestine samples of *Villin-Cre; Mapk14$^{f/f}$* mice. (b). *Mapk14* deficiency rescued villus premature aging and led to overgrowth of villus/crypt in *Villin-Cre; Tsc1$^{f/f}$* mice at 8 months of age. The decrease in the number of villi was due to fusion of the villi. Bottom panels: quantitation data (mean ± SEM). N=5 mice per group. **p<0.01 (determined using Student's *t*-test).

# Supplementary Figure 9

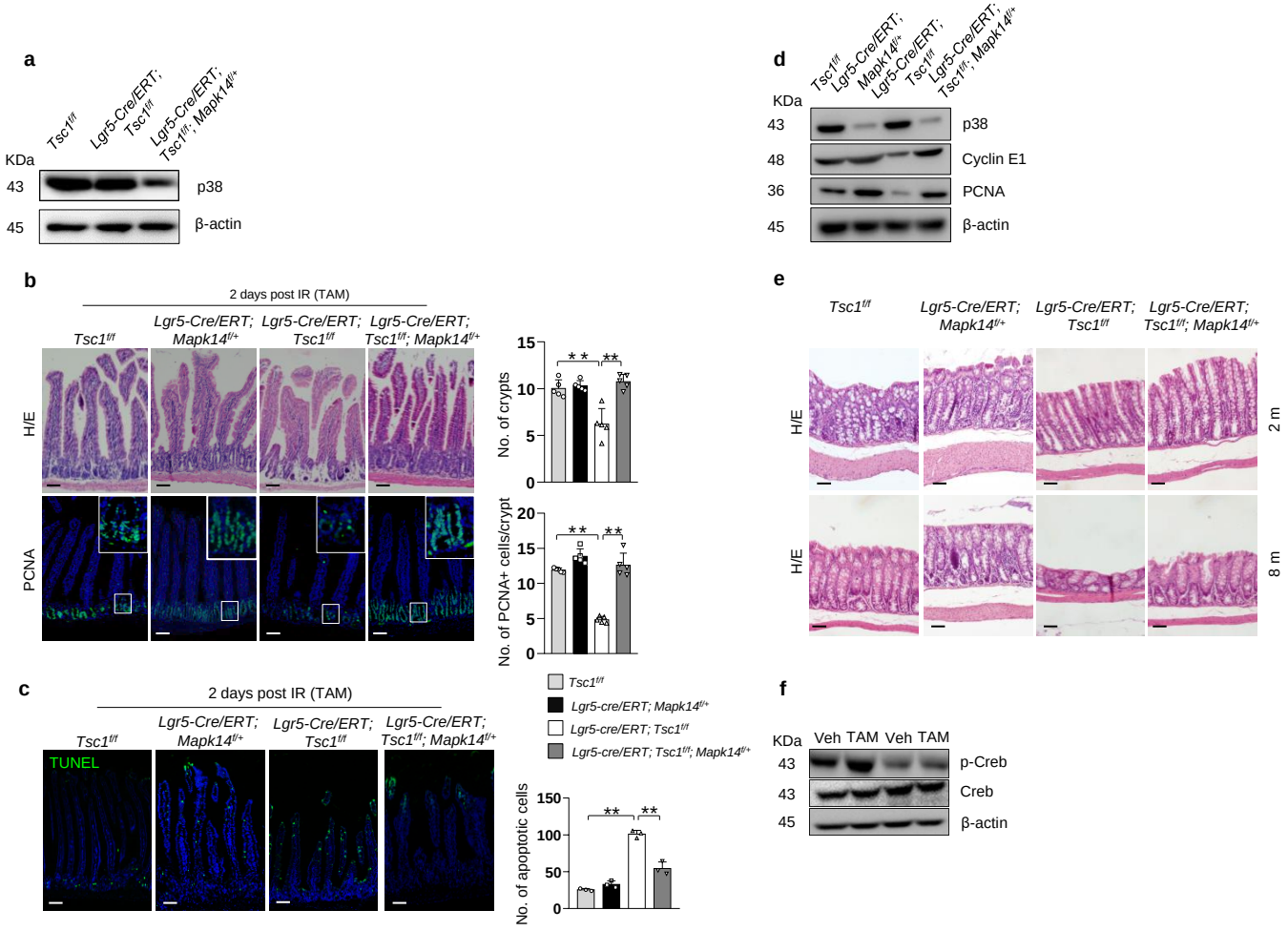


**Supplementary Figure 9. p38 MAPKs mediate the pro-aging effects of mTORC1 in *Lgr5-CreER; Tsc1$^{f/f}$* mice.**
(a). Western blot analysis revealed that p38α was deleted in crypt samples of *Lgr5-CreERT; Mapk14$^{f/+}$* mice. (b). *Mapk14* haplo-deficiency rescued the increased sensitivity to IR-induced decreases in the numbers of crypts and proliferating cells at day 2 post IR. Right panels: quantitation data (mean ± SEM). N=5 mice per group. **p<0.01 (determined using Student's *t*-test). (c). *Mapk14* haplo-deficiency rescued the increase in apoptotic cells 2 days after IR in *Lgr5-CreERT; Tsc1$^{f/f}$* mice. Bottom panels: quantitation data (mean ± SEM). N=3 mice per group. **p<0.01(determined using Student's *t*-test). (d). *Mapk14* haplo-deficiency rescued the decreases in PCNA and cyclin E and increase in p53 in crypt samples of *Lgr5-Cre/ERT; Tsc1$^{f/f}$* mice. (e). *Mapk14* haplodeficiency partially rescued colon crypt atrophy of *Lgr5-Cre/ERT; Tsc1$^{f/f}$* mice at 8 months of age. (f). SB203580 (SB) inhibited p38 MAPK activation, with p-Creb as an indicator. The mice were treated with SB203580 daily.

Supplementary Figure 10

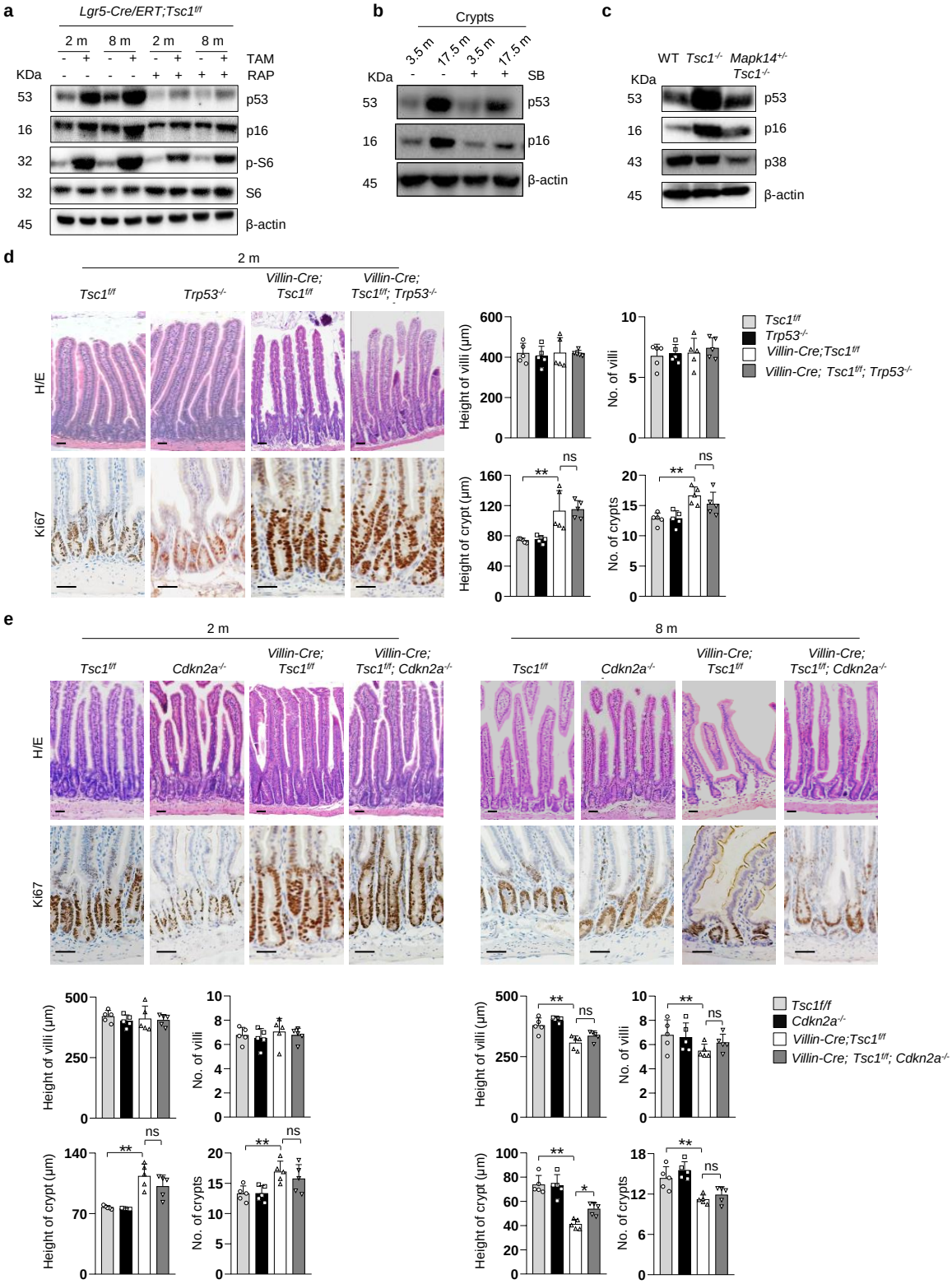


**Supplementary Figure 10. The different effects of p53 and p16 on mTORC1-driven villus aging.**
(a). Western blot results showed that *Tsc1* deletion induced an increase in the protein levels of p53 and p16 in crypt samples, which were suppressed by RAP. (b). Western blot results revealed that 17.5-month-old mice showed an increase in the levels of p53 and p16 in the crypts, which were suppressed by treating the mice with SB203580. (c). *Mapk14* haplo-deficiency suppressed the elevation of p53 and p16 in crypt samples of *Lgr5-CreERT; Tsc1$^{f/f}$* mice. (d). H/E staining of intestine sections of 2-month-old *Villin-Cre; Tsc1$^{f/f}$, Trp53$^{-/-}$*, and *Villin-Cre; Tsc1$^{f/f}$; Trp53$^{-/-}$* mice. Right panels: quantitation data (mean ± SEM). N=5. **p<0.01 (determined using Student's *t*-test). (e). H/E staining of intestine sections of 2- and 8-month-old *Villin-Cre; Tsc1$^{f/f}$, Cdkn2a$^{-/-}$* mice, and *Villin-Cre; Tsc1$^{f/f}$; Cdkn2a$^{-/-}$* mice. Bottom panels: quantitation data (mean ± SEM). N=4 mice per group. *p<0.05, **p<0.01 (determined using Student's *t*-test).

**Supplementary Figure 11. Uncropped western blot images.**

**Fig. 1g**

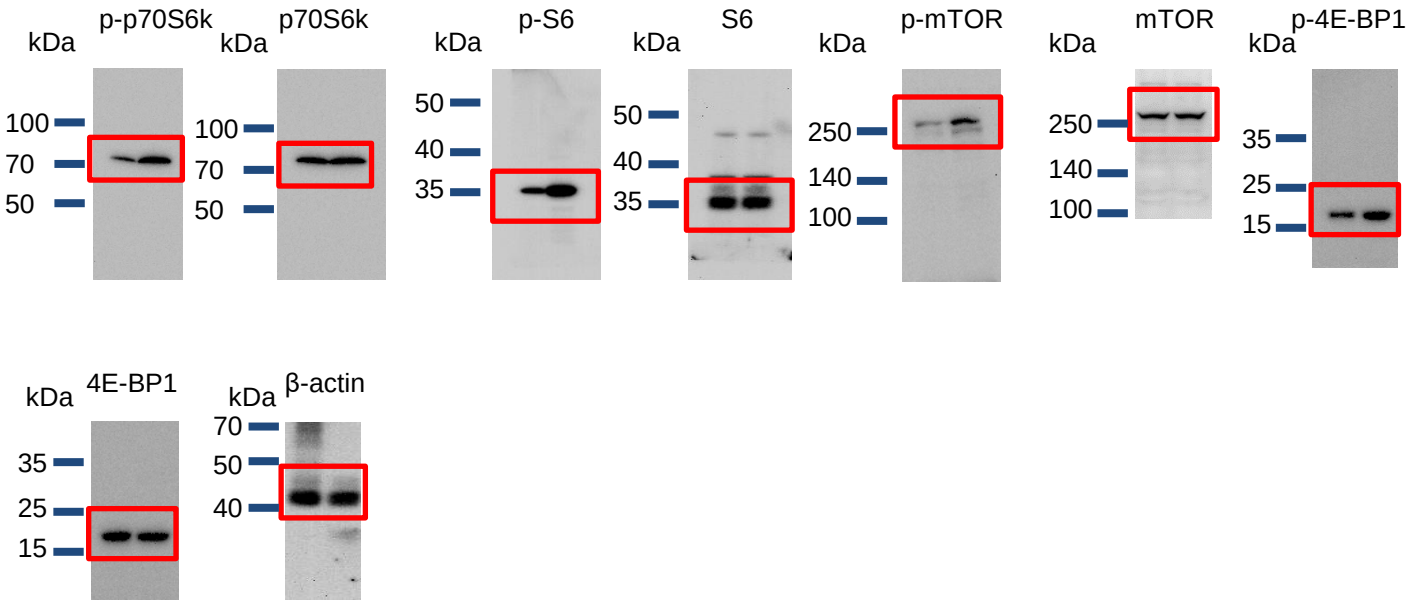

**Fig. 4a**

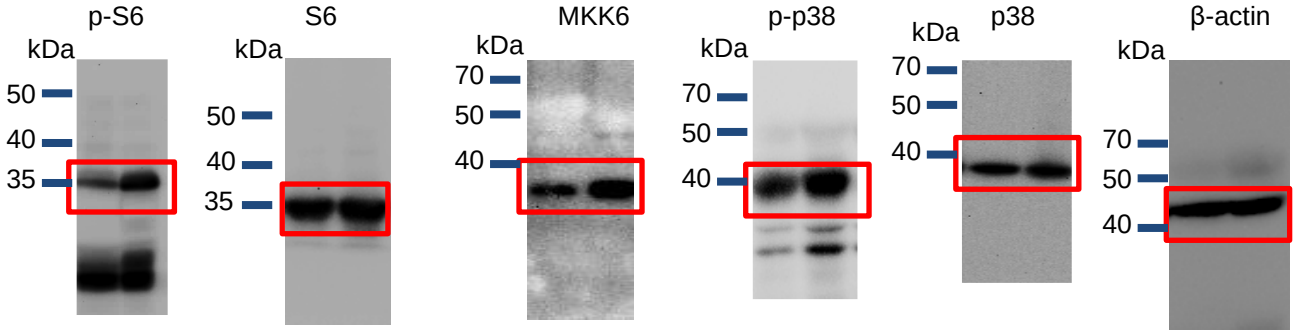


**Fig. 4b**

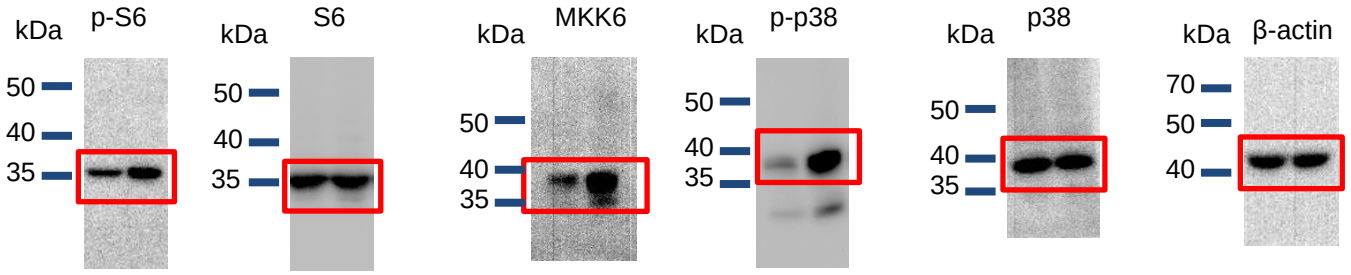


**Fig. 4d**

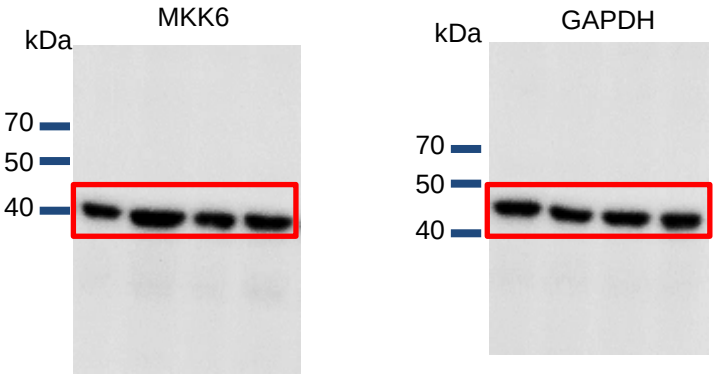


**Fig. 4e**

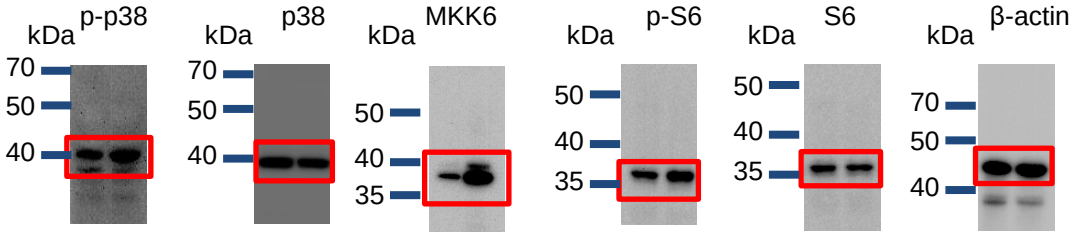

**Fig. 6a**

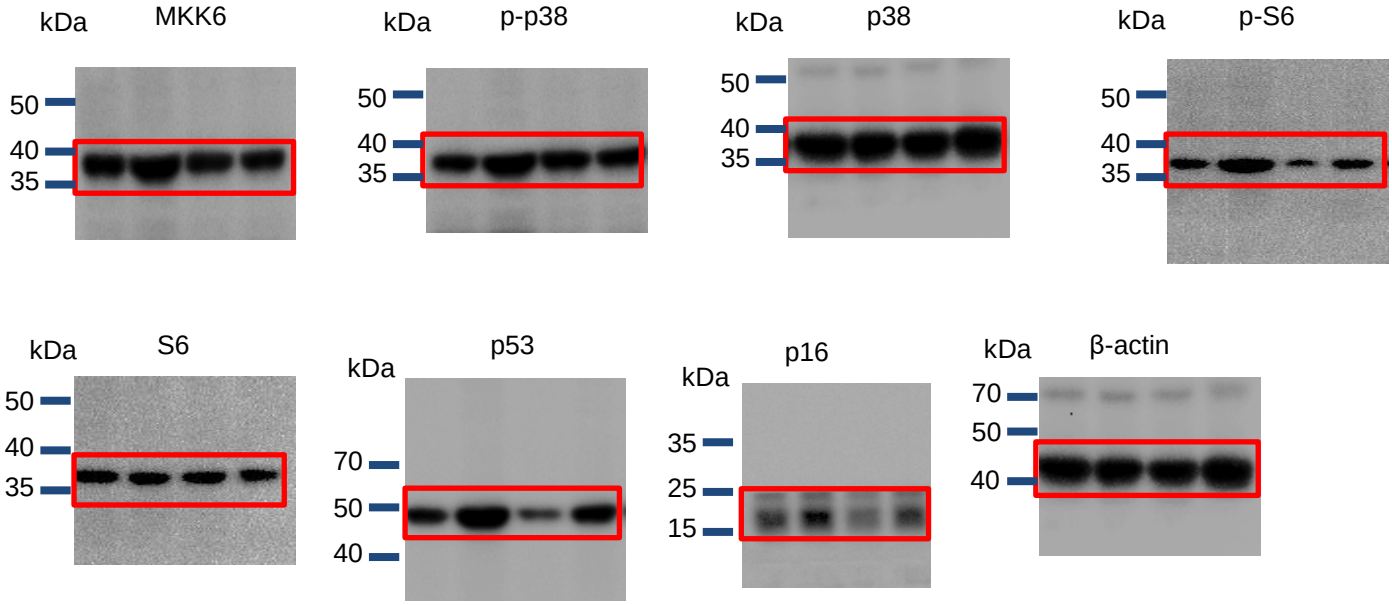
kDa
MKK6
50
40
35
kDa
p-p38
50
40
35
kDa
p38
50
40
35
kDa
p-S6
50
40
35
kDa
S6
50
40
35
kDa
p53
70
50
40
kDa
p16
35
25
15
kDa
β-actin
70
50
40

**Supplementary Fig. 2b**

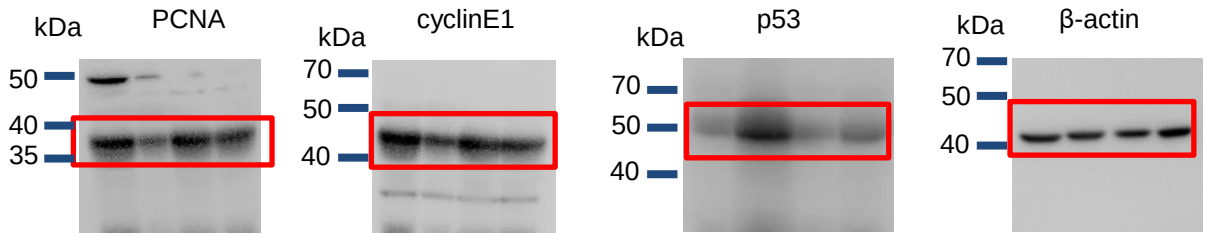


**Supplementary Fig. 5c**

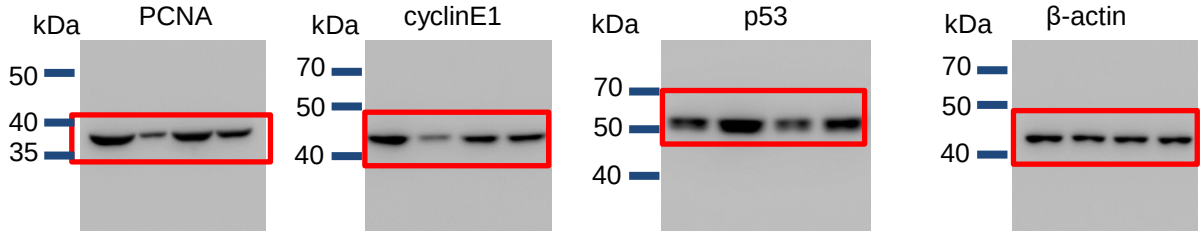

**Supplementary Fig. 7a**

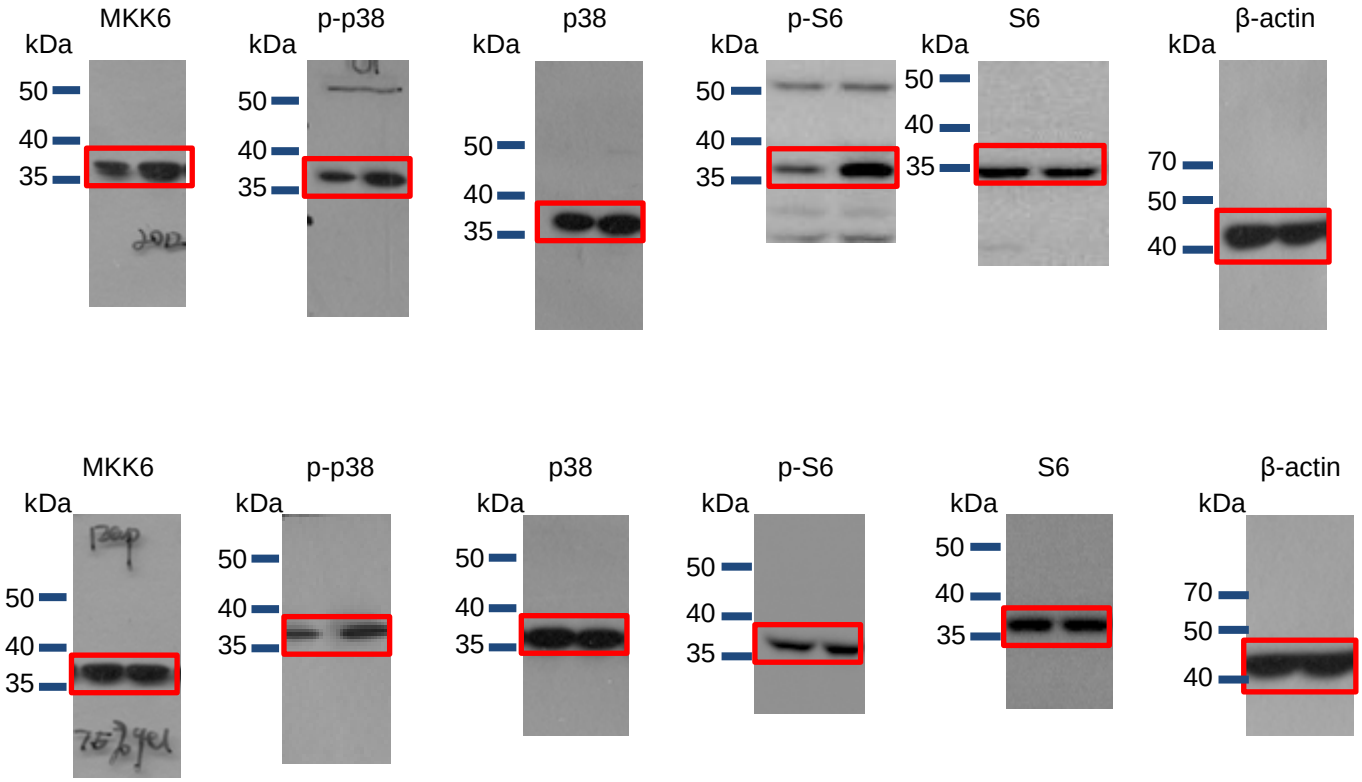


**Supplementary Fig. 7c**

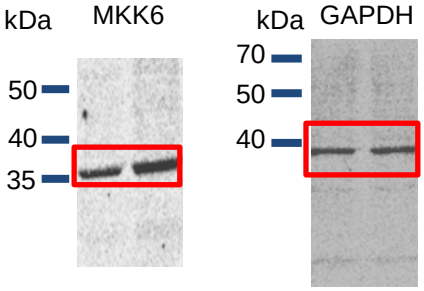


**Supplementary Fig. 7d**

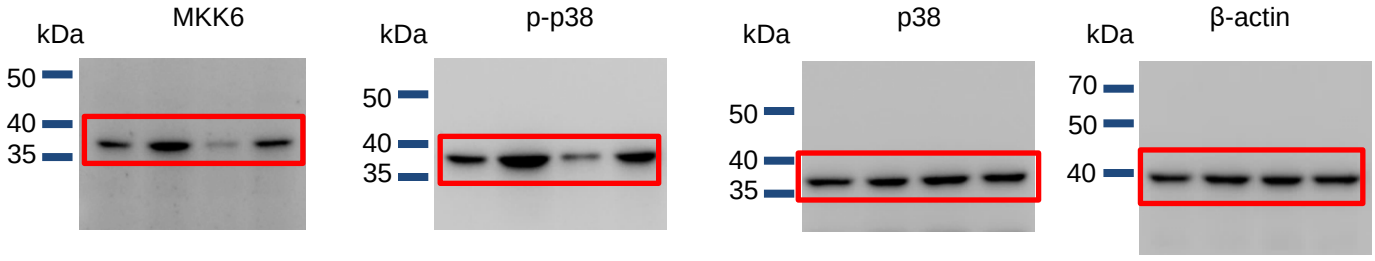

**Supplementary Fig. 8a**

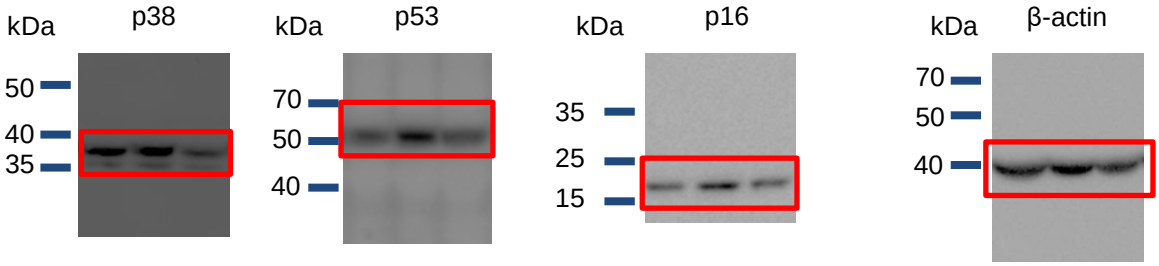

**Supplementary Fig. 9a**

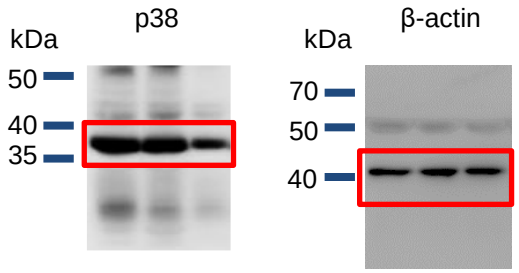


**Supplementary Fig. 9d**

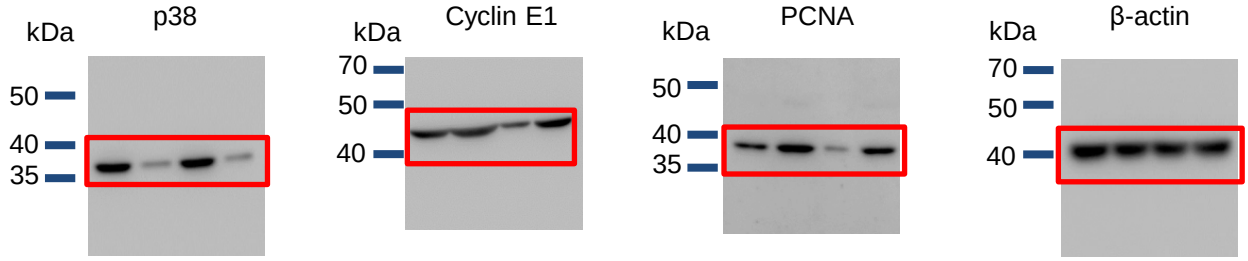


**Fig. s9f.**

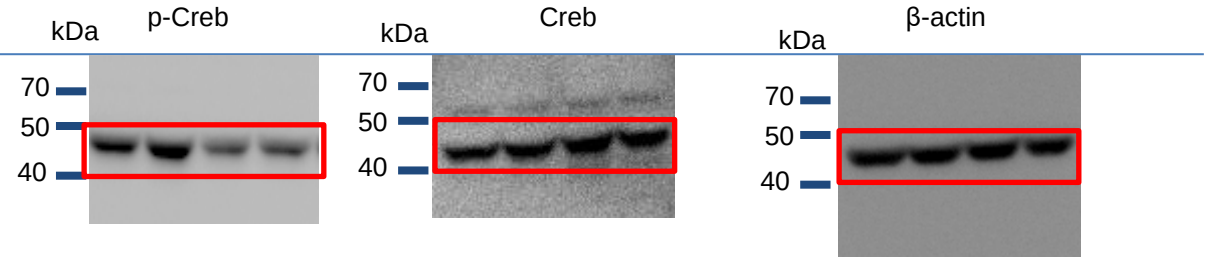

**Supplementary Fig. 10a**

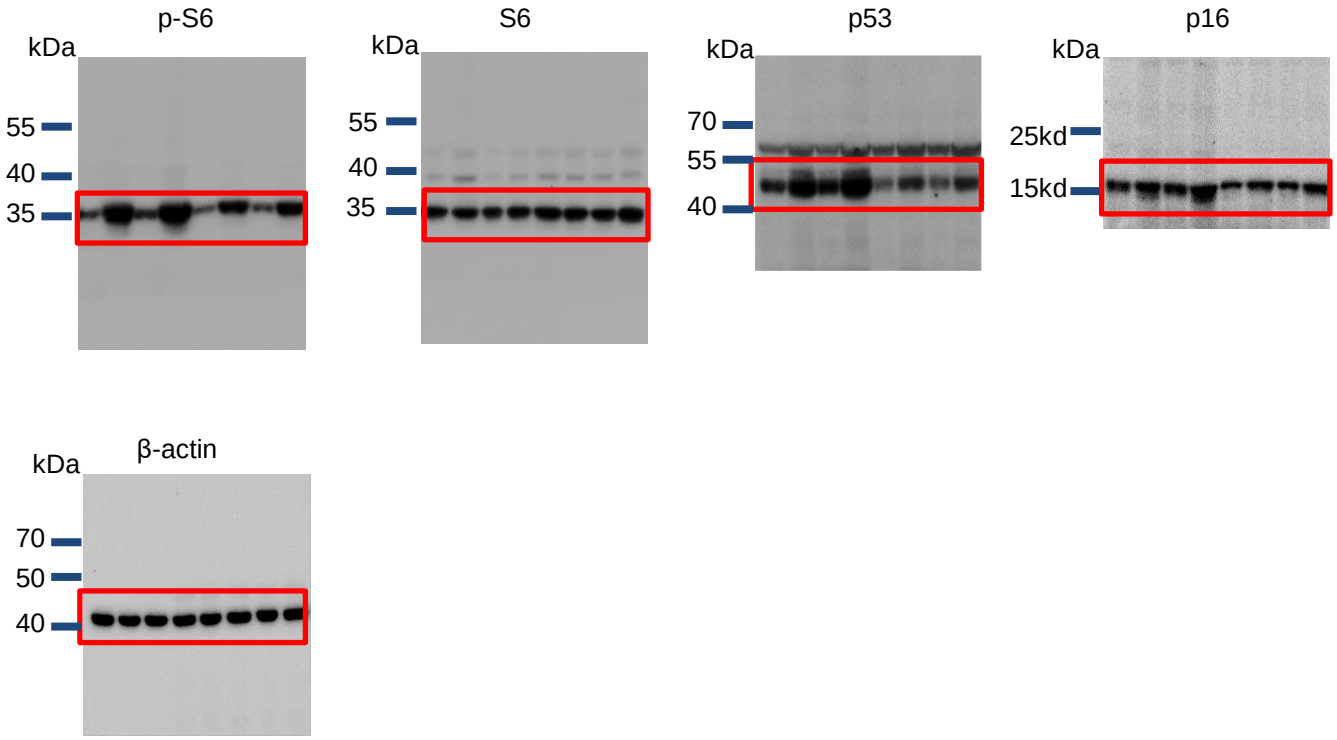


**Supplementary Fig. 10b**

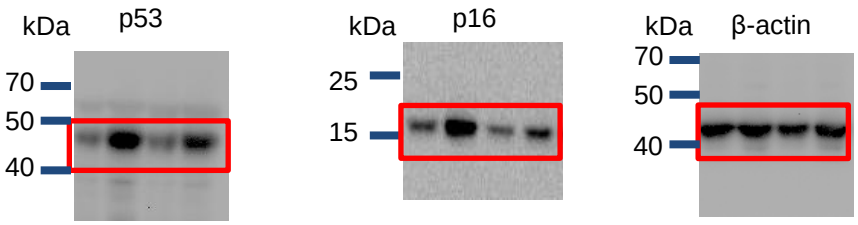


**Fig. s10c.**

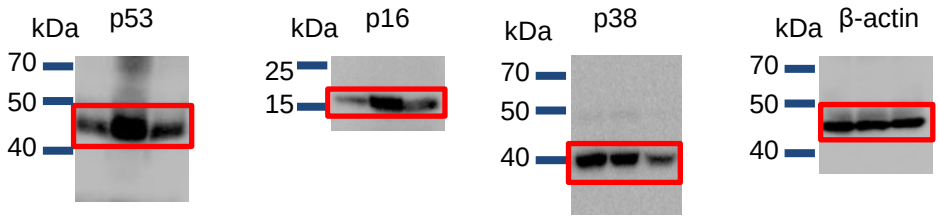

## Supplementary Table 1

| Protein List | Signals (WT) | Signals (KO) | KO/WT | |
|---|---|---|---|---|
| ATRIP (Ab-68/72) | 676.50 | 2344.33 | 3.47 | |
| Bax (N-term) | 351.00 | 553.83 | 1.58 | |
| BCL-2 (Phospho-Ser87) | 133.33 | 212.33 | 1.59 | |
| Beta actin | 168.50 | 280.00 | 1.66 | |
| BRCA1 (Ab-1423) | 3750.50 | 10391.67 | 2.77 | |
| Caspase-3 (Phospho-Ser150) | 137.60 | 213.67 | 1.55 | |
| CDK2 (Ab-160) | 136.00 | 245.67 | 1.81 | |
| Chk1 (Ab-286) | 180.83 | 420.33 | 2.32 | |
| Chk1 (Ab-317) | 128.83 | 296.17 | 2.30 | |
| Chk2 (Ab-383) | 266.67 | 406.33 | 1.52 | |
| Chk2 (Ab-68) | 369.33 | 2164.50 | 5.86 | |
| Chk2 (Phospho-Ser516) | 144.83 | 228.83 | 1.58 | |
| Cyclin D1 (ab-286) | 837.00 | 1610.60 | 1.92 | |
| Cyclin D1 (Ab-90) | 219.33 | 374.83 | 1.71 | |
| Cyclin D1 (Phospho-Thr286) | 237.17 | 735.00 | 3.10 | |
| Cyclin E1 (Ab-77) | 1691.40 | 3589.40 | 2.12 | |
| DNA-PK (Ab-2638) | 178.83 | 370.83 | 2.07 | |
| E2F1 (Ab-433) | 323.50 | 1301.17 | 4.02 | |
| ERK3 (Phospho-Ser189) | 125.20 | 191.17 | 1.53 | |
| HDAC1 (Ab-421) | 5833.50 | 11575.67 | 1.98 | |
| HDAC1 (Phospho-Ser421) | 187.40 | 309.33 | 1.65 | |
| HDAC2 (Phospho-Ser394) | 196.50 | 363.33 | 1.85 | |
| HDAC3 (Ab-424) | 261.33 | 703.33 | 2.69 | |
| HDAC4 (Phospho-Ser632) | 158.00 | 263.67 | 1.67 | |
| HDAC5 (Phospho-Ser259) | 154.50 | 260.00 | 1.68 | |
| HDAC5 (Phospho-Ser498) | 117.80 | 188.83 | 1.60 | |
| MAPKAPK2 (Ab-272) | 125.50 | 190.67 | 1.52 | |
| MAPKAPK2 (Phospho-Ser272) | 186.67 | 424.00 | 2.27 | |
| MDM2 (Ab-166) | 4277.83 | 11611.00 | 2.71 | |
| MEK1 (Ab286) | 505.33 | 1800.67 | 3.56 | |
| MEK1 (Ab-291) | 167.20 | 375.83 | 2.25 | |
| MEK1 (Ab-298) | 573.17 | 2611.50 | 4.56 | |
| p38 MAPK (Ab-182) | 576.00 | 4153.17 | 7.21 | |
| p53 (Ab-18) | 161.40 | 420.00 | 2.60 | |
| p53 (Ab-20) | 839.60 | 2073.50 | 2.47 | |
| p53 (Ab-33) | 184.67 | 379.20 | 2.05 | |
| p53 (Ab-37) | 166.00 | 266.83 | 1.61 | |
| p53 (Ab-392) | 202.17 | 303.50 | 1.50 | |
| Positive Marker | 8036.20 | 12036.60 | 1.50 | |
| Raf1 (Ab-341) | 138.83 | 219.50 | 1.58 | |
| Rb (Ab-780) | 177.40 | 382.00 | 2.15 | |
| Rb (Ab-795) | 162.17 | 485.67 | 2.99 | |
| Rb (Ab-807) | 207.00 | 545.60 | 2.64 | |
| RBAK (inter) | 133.40 | 625.33 | 4.69 | |
| RBM5 (inter) | 162.00 | 2247.20 | 13.87 | |
| | | | | |

**Supplementary Table 1. Increased expression and activation of molecules involved in proliferation in intestine samples.** Proteins with KO/WT ratios greater than 1.5 were shown.